Frequency modulation of neural oscillations according to visual task demands

Andreas Wutz[a,b,1,2], David Melcher[a], and Jason Samaha[c,1,2]

[a]Center for Mind and Brain Sciences, University of Trento, I-38068 Rovereto, Italy; [b]The Picower Institute for Learning and Memory, Department of Brain and Cognitive Sciences, Massachusetts Institute of Technology, Cambridge, MA 02139; and [c]Department of Psychology, University of Wisconsin–Madison, Madison, WI 53706

Edited by Ranulfo Romo, Universidad Nacional Autonóma de México, Mexico City, D.F., Mexico, and approved December 22, 2017 (received for review July 26, 2017)

Temporal integration in visual perception is thought to occur within cycles of occipital alpha-band (8–12 Hz) oscillations. Successive stimuli may be integrated when they fall within the same alpha cycle and segregated for different alpha cycles. Consequently, the speed of alpha oscillations correlates with the temporal resolution of perception, such that lower alpha frequencies provide longer time windows for perceptual integration and higher alpha frequencies correspond to faster sampling and segregation. Can the brain's rhythmic activity be dynamically controlled to adjust its processing speed according to different visual task demands? We recorded magnetoencephalography (MEG) while participants switched between task instructions for temporal integration and segregation, holding stimuli and task difficulty constant. We found that the peak frequency of alpha oscillations decreased when visual task demands required temporal integration compared with segregation. Alpha frequency was strategically modulated immediately before and during stimulus processing, suggesting a preparatory top-down source of modulation. Its neural generators were located in occipital and inferotemporal cortex. The frequency modulation was specific to alpha oscillations and did not occur in the delta (1–3 Hz), theta (3–7 Hz), beta (15–30 Hz), or gamma (30–50 Hz) frequency range. These results show that alpha frequency is under top-down control to increase or decrease the temporal resolution of visual perception.

visual perception | temporal integration | alpha oscillations | oscillation frequency | top-down control

Visual perception is tasked both with constructing stable representations over time as well as maximizing sensitivity to transient changes. A large body of work has shown that neural oscillations in the alpha band (8–12 Hz) are partially responsible for determining the temporal resolution of perception, such that when discrete events occur within the same oscillatory cycle they can become perceptually integrated (1–8). For instance, individuals with higher peak alpha frequencies have perception with higher temporal resolution (2, 9), indicating that lower peak frequencies correspond to integration over longer time windows. Furthermore, trial-to-trial variability in spontaneous alpha frequency predicts accuracy in a temporal discrimination paradigm (9) and the rate of illusory flicker (10).

These findings raise the question of whether variability in peak alpha frequency is stochastic, varying randomly across persons and fluctuating over time within the same person, or might instead be strategically modulated based on task demands. It is known that the temporal resolution of visual perception can be modulated by attention (11–13), and oscillatory phase and power can be controlled by top-down factors (14–18). Here, we investigated whether the peak frequency of alpha oscillations is subject to attentional control, increasing or decreasing so as to effectively lengthen or shorten the temporal window of perceptual integration.

To examine this question, we recorded magnetoencephalography (MEG) data while observers performed two different tasks, one requiring visual integration over time and the other involving visual segregation over time. Both tasks are variants of a classical perceptual integration paradigm called the missing-element task (MET) (19). In the MET, an array of elements is presented in two successive frames, separated by a short interstimulus interval (ISI). When superimposed, the elements in both frames occupy all but one of the positions in the array and the observer's job is to identify the position with the missing element (Fig. 1*A*, blue). As ISI decreases, the two frames become perceptually integrated and identifying the missing element is simple. We introduced another condition that we term the odd-element task (OET) (20). In the OET, one-half of one of the elements is presented in the first frame and the other half is presented in the second (Fig. 1*A*, red). Here, the observer's task is to decide which location contained this odd element, which becomes easier as ISI increases and the frames are perceptually segregated. Critically, the use of these two tasks allowed us to determine whether modulations of peak alpha frequency were specifically tied to temporal resolution, as opposed to a more general fluctuation in attention or in visual sensitivity or criterion (21, 22). We hypothesized that if frequency modulation of alpha supports top-down control over temporal integration, then we should observe higher frequencies during the OET (when segregation is beneficial) compared with the MET (when integration is beneficial).

Results

By mapping psychometric functions relating performance on both tasks to ISI (sigmoid fit $R^2 = 0.94$ for OET, $R^2 = 0.93$ for MET), we could identify intersection points for each observer

Significance

Neural oscillations are hypothesized to play an important role in modulating perceptual processing in accordance with top-down goals. For instance, the amplitude, phase, and spatial distribution of alpha-band oscillations change with attention. Given recent links between the peak frequency of alpha oscillations and the temporal resolution of perception, we investigated whether frequency modulation occurs when task demands emphasize integration or segregation of visual input over time. We found that alpha frequency in occipital–temporal cortex decreased during, and in anticipation of, stimulus processing when task demands required temporal integration compared with segregation. These results demonstrate a unique top-down mechanism by which the brain controls the temporal resolution of visual processing in accordance with current task demands.

Author contributions: A.W., D.M., and J.S. designed research; A.W. performed research; J.S. contributed new reagents/analytic tools; A.W. analyzed data; and A.W., D.M., and J.S. wrote the paper.

The authors declare no conflict of interest.

This article is a PNAS Direct Submission.

[1]A.W. and J.S. contributed equally to this work.

[2]To whom correspondence may be addressed. Email: awutz@mit.edu or jsamaha@wisc.edu.

This article contains supporting information online at www.pnas.org/lookup/suppl/doi:10.1073/pnas.1713318115/-/DCSupplemental.

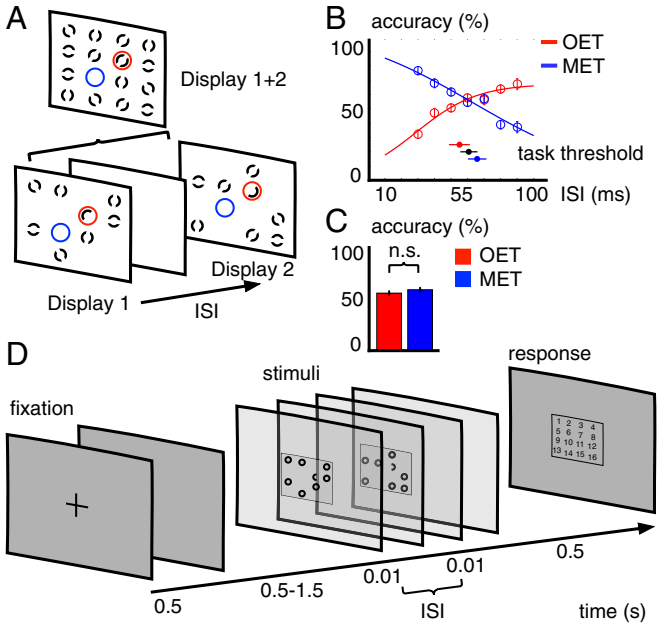

Fig. 1. Task and behavioral data. (*A*) Stimuli for the missing/odd-element task (MET/OET). (*B*) Behavioral data for the psychophysical threshold assessment. Lines show the sigmoid fit. Inset circles show the 50% threshold of the sigmoid fit for each task (red, blue) and the between-task intersection point (black). Error bars show ±1 SE. (*C*) Behavioral data during MEG recording. (*D*) Trial sequence.

where the same ISI produced the same performance across tasks (Fig. 1*B*; mean ± SD, 61 ± 22 ms). This allowed us to equate performance [Fig. 1*C*; mean ± SD, 55 ± 11% correct for OET, 58 ± 11% for MET; $t_{(18)} = -1$; $P = 0.35$] and use the same physical stimuli, while manipulating only whether perceptual integration or perceptual segregation was required for task performance (MET and OET, respectively).

We analyzed whole-brain MEG data from 19 observers while they performed separate blocks of the OET and MET with an ISI fixed at a psychometric intersection point determined before MEG acquisition (Fig. 1*B*). The signal at each MEG sensor was bandpass filtered for alpha (8–12 Hz) and the phase angle time series was extracted via Hilbert transform (*Materials and Methods*). The temporal derivative of the phase angle time series was computed as an index of the instantaneous frequency of the band-limited signal (9, 23). In support of our hypothesis, we found a significant ($P < 0.002$, cluster corrected) spatiotemporal cluster of higher alpha frequencies during the OET than during the MET (Fig. 2 *A* and *B*). Significant frequency modulation emerged 360 ms before stimulus onset, suggesting a preparatory top-down effect, and lasted for 500 ms afterward (Fig. 2 *A* and *C*). We observed this effect both in induced alpha activity (Fig. 2) and in the evoked alpha response ($P < 0.022$, cluster corrected; Fig. S1). Oscillatory power during this timeframe was not reliably modulated by task (after correction for multiple comparisons) but was primarily restricted to the alpha and beta band (Fig. S2).

To verify the results of the instantaneous frequency analysis while taking into account individual variability in peak alpha frequency, we conducted a separate fast Fourier transform (FFT) analysis of prestimulus and poststimulus time windows (−0.5–0 and 0–0.5 s). Alpha peaks averaged over the significant sensors from the instantaneous frequency analysis (Fig. 2*B*) varied between 8.7 and 14.7 Hz (Figs. S3 and S4). [Note that the difference in frequency estimated from the instantaneous frequency analysis (∼9.9 Hz; Fig. 2*A*) and the FFT peak detection analysis (∼11.1 Hz; Fig. 3*A*) results from the fact that the data were filtered into an a priori band of 8–12 Hz for the instantaneous frequency analysis, whereas the FFT peak detection analysis searched a large window of 8–15 Hz. Repeating the instantaneous frequency analysis with an 8- to 15-Hz bandpass filter did not change the frequency modulation effect, and the resulting frequency estimates were more closely aligned between the two analyses (Fig. S9).] Critically, a 2 × 2 repeated-measures ANOVA revealed a main effect of task (OET, MET: $F_{(1,18)} = 10.7$, $P < 0.005$) and interval (pre, post: $F_{(1,18)} = 5.5$, $P < 0.03$) on peak alpha frequency, with no interaction ($P = 0.42$; Fig. 3*A*). Paired *t* tests indicate that both prestimulus [$t_{(18)} = 2.44$, $P < 0.026$] and poststimulus [$t_{(18)} = 2.36$, $P < 0.03$] alpha peaked at a lower frequency during the MET. These results confirm the instantaneous frequency finding and indicate that the prestimulus result is not an artifact of temporal smoothing in the analysis.

We used a linear constrained minimum variance (LCMV)-beamforming algorithm (*Source Localization*) to localize the neural generators of the observed, sensor-level effects. Given the visual nature of the task and prior expectations about the significance of alpha in visual cortex (24), we investigated a region of interest (ROI) defined from bilateral early visual (calcarine) cortex. A 2 × 2 repeated-measures ANOVA revealed a main effect of task (OET, MET) on alpha frequency [$F_{(1,18)} = 7.15$, $P < 0.016$], with no effect of hemisphere ($P > 0.07$) and no interaction ($P > 0.85$), in early visuocortical source estimates (Fig. 3*B*). To test for a potential contribution of motor-cortical alpha rhythms, we also contrasted alpha frequencies in bilateral primary and supplementary

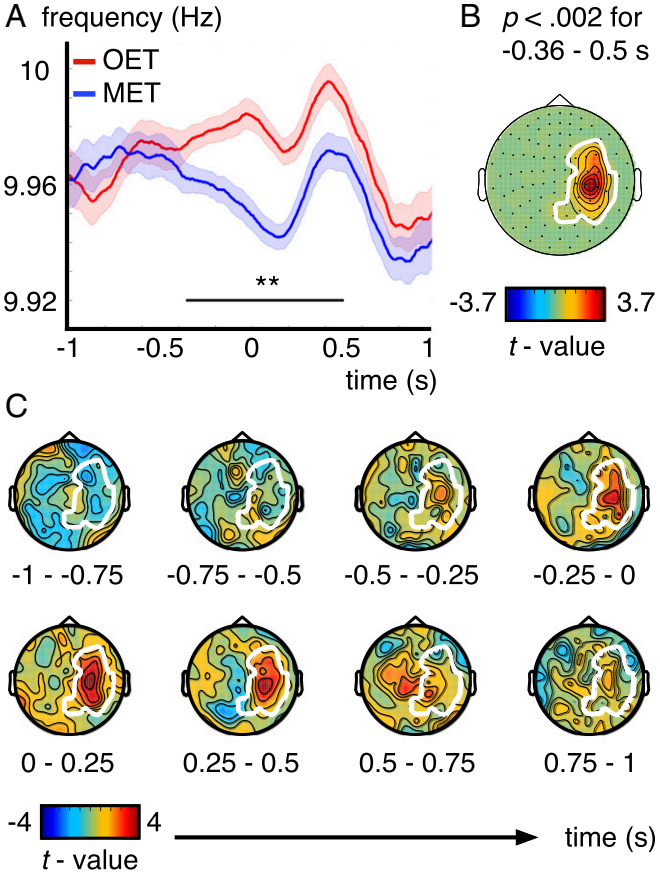

Fig. 2. Instantaneous alpha frequency. (*A*) Instantaneous frequency in the alpha band over time (relative to display 1 onset) averaged over significant channels (shown in *B*). Shaded areas show ±1 SE. The horizontal line shows the significant time epoch. Asterisks indicate the significance level (with $^{**}P < 0.01$, sensor-time cluster corrected). (*B*) MEG-sensor topography averaged over the significant time epoch (shown in *A*) for the contrast OET vs. MET. Nonsignificant channels are masked. (*C*) MEG-sensor topographies (OET vs. MET) over time in steps of 0.25 s. The white outline shows significant channels for the time epoch from −0.36 to 0.5 s.

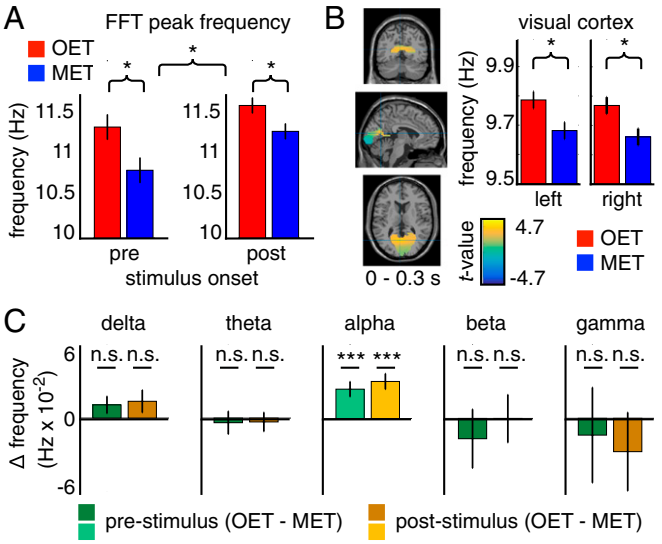

Fig. 3. Prestimulus/poststimulus peak frequency, neural source, and frequency specificity. (*A*) Alpha peaks with FFT analysis averaged over the channels of interest (Fig. 2*B*) for prestimulus (−0.5–0 s, *Left*) and poststimulus time epochs (0–0.5 s, *Right*). (*B*) Source localization in visual cortex (ROI) for the contrast OET vs. MET averaged between 0 and 0.3 s. Bar plots show source-localized alpha frequency by visuocortical hemisphere and task. (*C*) Difference (OET − MET) in instantaneous frequency in the delta (1–3 Hz), theta (3–7 Hz), alpha (8–12 Hz), beta (15–30 Hz), and gamma bands (30–50 Hz) averaged between −0.3 and 0 s (prestimulus) or 0 and 0.3 s (poststimulus) and over the channels of interest (Fig. 2*B*). Error bars show ±1 SE. Asterisks indicate the significance level (with n.s. indicating not significant, $*P < 0.05$, $***P < 0.001$).

motor cortex (Fig. S5*B*), which revealed no main effect of task or interactions with hemisphere (all values of $P > 0.41$).

To ensure that we did not miss other important effects with our ROI analysis, we additionally ran a whole-brain contrast. Constraining activations to extend a minimum of at least two adjacent significant voxels ($P < 0.05$, uncorrected), we observed only two significant clusters. One bilaterally in visual cortex (maximum voxel in cluster, left BA 17, MNI coordinates (mm) = [−5–65 10]; right BA 19, MNI (mm) = [55–65 10]) and one in the right inferior temporal gyrus (BA 37, MNI (mm) = [55–50 −20]; Fig. S5*A*). This suggests a contribution of right-lateralized inferotemporal regions, in addition to bilateral early visual cortex, which may underlie the lateralization evident in the sensor topography.

A number of oscillatory frequencies have been linked to temporal and perceptual processing, in general. For example, theta-band rhythms have been claimed to segment inputs into semantic temporal chunks (20, 25), whereas beta and gamma oscillations may mediate the interplay between bottom-up, sensory processing and top-down control (26, 27). We reconducted the instantaneous frequency analysis (Fig. 2) but with data filtered into different canonical frequency bands. Averaging over prestimulus (−0.3–0 s) and poststimulus (0–0.3 s) windows (where the alpha effect was maximal), we found that the task-related modulation of peak frequency was specific to alpha [pre: $t_{(18)} = 3.92$, $P < 0.001$; post: $t_{(18)} = 4.75$, $P < 0.0002$ Fig. 3*C*]. There was no significant difference in the delta, theta, beta, or gamma bands, either prestimulus or poststimulus, when tested in the channel group of interest (all $P > 0.13$) or across all MEG sensors (all $P > 0.19$, cluster corrected).

To relate alpha frequency modulation to behavior, we examined instantaneous frequency for each task as a function of trial accuracy (correct or incorrect). We observed frequency modulation for both correct (−0.27–0.13 s, $P < 0.012$, cluster corrected) and incorrect trials (−0.07–0.48 s, $P < 0.004$, cluster corrected, Fig. 4*A*), but correct trials were associated with an earlier onset of frequency modulation. We formally tested this by contrasting OET > MET instantaneous frequency across trials for each subject individually and extracting the earliest onset of a significant difference ($P < 0.05$, or the smallest P value in the case of subjects with no significant differences; *MEG Data Analysis*). Fifteen of 19 subjects had significantly higher alpha frequencies during the OET than the MET on correct trials, and 12 of 19 had a significant difference on incorrect trials, highlighting the reliability of the frequency modulation effect at the single-subject level. Importantly, the onset of significant frequency modulation occurred earlier on correct (mean = −0.45 s, relative to target onset), compared with incorrect trials (mean = −0.14 s; $z = -2.9$, $P < 0.004$, Wilcoxon signed rank test; Fig. 4*A*, *Bottom*).

Variability in instantaneous alpha frequency across subjects was marginally predictive of behavioral thresholds (ISI with 50% correct responses) for the OET, in accordance with previous findings (2, 9), indicating that subjects with higher alpha frequencies can segregate stimuli over shorter temporal windows ($r = -0.47$, $P < 0.066$; 0.17–0.27 s, time-cluster corrected; Fig. 4*B*). A similar trend was not present, however, between alpha frequency and MET thresholds (Fig. S7). This is perhaps unsurprising given that OET and MET thresholds were themselves not reliably correlated across subjects ($r = 0.20$, $P > 0.42$), which likely indicates that additional factors beyond the temporal resolution of perception contribute to difficulty for each task (e.g., contrast, crowding). Interestingly, we also observed a strong positive correlation between the magnitude of change in alpha frequency (OET − MET) and perceptual thresholds for the MET ($r = 0.62$, $P < 0.002$; 0.2–0.5 s, time-cluster corrected). Subjects who could modulate alpha frequency more strongly could also integrate over longer temporal windows (see Fig. S7 for the temporal evolution of these correlations).

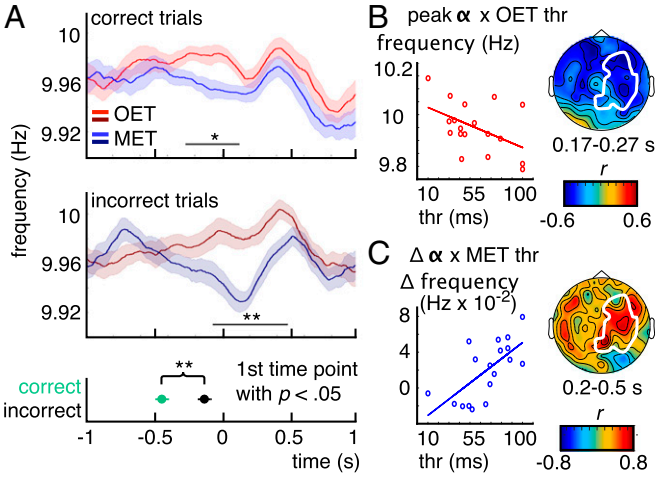

Fig. 4. Correct vs. incorrect trials and correlations between instantaneous alpha frequency and behavior. (*A*) Instantaneous frequency in the alpha band averaged over the channels of interest (Fig. 2*B*) for correct (*Upper*) and incorrect trials (*Middle*). The *Lower* shows the average first significant time point during correct (green) and incorrect trials (black). Shaded areas show ±1 SE. The horizontal lines show the significant time epoch. Asterisks indicate the significance level (with $*P < 0.05$, $**P < 0.01$, time-cluster corrected). (*B*) Each subject's alpha frequency averaged over the time epoch (0.17–0.27 s; Fig. S7) and the channels of interest (Fig. 2*B*) plotted against the ISI that yielded 50% correct trials in the OET. Line shows the linear fit. (*Right*) MEG-sensor topography for the correlation between 0.17 and 0.27 s. The white outline shows the channels of interest. (*C*) Each subject's difference in instantaneous alpha frequency between tasks (OET − MET) averaged over the time epoch (0.2–0.5 s; Fig. S7) and the channels of interest (Fig. 2*B*) plotted against the ISI that yielded 50% correct trials in the MET. Line shows the linear fit. (*Right*) MEG-sensor topography for the correlation between 0.2 and 0.5 s.

Discussion

We contrasted neural activity during two tasks with identical stimulus displays and matched difficulty that varied in their instructions to either integrate or segregate the stimuli over time. We found the frequency of neural oscillations in the alpha band differed between these tasks, such that alpha frequencies increased when task demands required temporal segregation compared with integration. These results suggest that alpha frequencies can "speed up" when task demands require that visual information be sampled more frequently. Alternatively, alpha may "slow down" when information needs to be combined over longer timescales. The direction of this effect—faster alpha for segregation and slower alpha for integration—is predicted by current theories, which postulate that alpha oscillations are critically involved in determining the temporal resolution of perceptual processing by integrating over inputs occurring within the same oscillatory cycle (reviewed in ref. 7). This finding constitutes an instance of top-down control over the frequency of alpha oscillations, revealing a unique mechanism for dynamically controlling the temporal resolution of visual perception.

By analyzing the instantaneous frequency of oscillations in the alpha band, we observed the temporal dynamics of top-down frequency modulation. This analysis indicated that alpha frequency modulation occurred in anticipation of the target stimulus and was sustained throughout stimulus processing. To rule out the possibility that the prestimulus result reflected a smearing of poststimulus differences into the prestimulus window (due to smoothing inherent in the analysis), we conducted an FFT analysis of alpha peaks based only on the prestimulus data. This analysis confirmed frequency modulation in the prestimulus window, which strongly suggests that alpha frequency is under endogenous control. Notably, frequency modulation was not sustained throughout the entire trial epoch. Instead, it was strategically timed just before target onset (and emerged ∼500 ms after trial onset; Fig. S8), suggesting that the underlying process involves dynamic control as opposed to a state change in peak frequency lasting for the entire duration of a task block. Furthermore, the onset of frequency modulation was predictive of behavior, such that correct trials were associated with an earlier onset modulation, underscoring the importance of preparatory frequency modulation for task performance.

Changes in oscillatory frequency have previously been explored in response to visual stimuli of varying luminance, where it was observed that alpha frequencies increase with increasing luminance (23). Alpha frequency has also been targeted with transcranial alternating current stimulation, which may exogenously drive alpha at higher or lower frequencies. This external stimulation, in turn, impacts the duration of cross-modal temporal integration windows (2), and illusory jitter perception of a moving stimulus (10), lending causal support to the relationship between alpha frequency and temporal integration. The present results indicate that alpha frequency can be controlled endogenously, and thereby also suggests a possible mechanism underlying the recent finding that the phase of alpha oscillations may be guided by top-down control (refs. 14 and 15; but see ref. 28). By fine-tuning oscillatory frequency over the course of learning, the phase of ongoing oscillations can be aligned to expected inputs in a top-down manner.

Consistent with previous effect sizes based on instantaneous frequency measurement (9, 23), the change in frequency we observed was small, on the order of 0.04 Hz. However, it is difficult to interpret this difference as the true effect size in the task-relevant neural population given that macroscopic measurements such as MEG and EEG measure a mixture of many neural sources. It is likely that only a fraction of the alpha generators contributing to the scalp signal are modulating in frequency, whereas others (for example, in motor cortex; Fig. S5) are not. The resulting sum of modulating and nonmodulated sources would make the observed effect at the scalp level much smaller than that present in the task-relevant neural populations. Consistent with this reasoning, source-level estimates of instantaneous alpha frequency in visual cortex (Fig. 3*C*) showed a mean difference between tasks about an order of magnitude larger than that observed on the scalp (Fig. 2*A*).

The precise neurophysiological mechanisms of endogenous control over alpha frequencies have not yet been explored. Recordings in the lateral geniculate nucleus (LGN) of the thalamus have led to the discovery of a specialized subset of thalamocortical neurons that burst at alpha frequencies. Those thalamic neurons synchronize through gap junctions to form an alpha pacemaker that is synchronized with scalp-recorded alpha oscillations (29–31). Importantly, relay-mode neurons in the LGN, which are thought to transmit information from retina to visual cortex, time their spiking in accordance with the phase of the alpha rhythm established by these pacemaker cells. This thalamocortical circuit provides a plausible neurophysiological basis for the link between alpha and perception (32). Alpha frequency modulation may therefore involve modulation of LGN pacemaker cells. One possibility might involve a multisynaptic feedback pathway linking goal representations in prefrontal cortex to the LGN via the thalamic reticular nucleus (33–35). Alternatively, cortical generators of alpha oscillations have also been proposed in a variety of regions including visual and inferotemporal cortex (36–38). These areas may interact with high-order regions to implement goal-directed control over visual processing through known cortico–cortico projections between prefrontal and parietal cortex (27, 39, 40). Our source localization results suggest a locus in primary visual and inferotemporal cortex, although evidence for a thalamic contribution would be difficult to detect with MEG and cannot be ruled out.

Our results provide an important step toward understanding the neurophysiological foundation of top-down alpha frequency modulation in the cortex. These findings inform our understanding of how the brain dynamically tunes up or down its perceptual processing speed to master the real-time demands of the visual environment.

Materials and Methods

All procedures were approved by the ethics committee of the University of Trento.

Participants. Nineteen participants (nine males; mean ± SD, 27 ± 4.7 y; 17 right-handed) took part in the experiment. All participants had normal or corrected-to-normal vision, gave written informed consent before the experiment, and received a monetary compensation. One subject was excluded from the correlation analysis (see *Behavioral Data Analysis* for details).

Stimuli. The stimulus display contained annuli placed within an invisible 4 × 4 quadratic element grid [3.5° degrees visual angle (DVA)]. Stimuli were shown over two different frames separated by a blank display (Fig. 1*A*). Seven random locations (14 over both frames out of 16 total) were occupied with a black annulus on a uniform gray background (0.5° DVA size, 0.06° DVA line width; 0.5° DVA evenly spaced between grid locations). Each annulus was split by a central gap with a randomly chosen orientation between 0°, 45°, 90°, and 135°. For segregation, an odd element on the display had to be detected (OET). The odd element was made up as either one-half of the annulus on one random display location. The partial annuli complement each other across displays. Thus, to recognize it as an odd element, the participants had to segregate the displays over time (Fig. 1*A*, red). For integration, the target was a missing element on the display (MET). To detect this empty location, the participants had to integrate information from both displays over the ISI (41) (Fig. 1*A*, blue). Both odd and missing elements were shown on each trial, but the participants were instructed to attend to and detect only one of the two targets and ignore the other in different blocks. Thus, the stimuli were physically identical in every block. The blocks only differed in terms of task instructions (order counterbalanced across subjects). The time between displays was set at a specific ISI for each subject. This ISI value was estimated by psychometric curve fitting before the MEG experiment (see below). Performance during recording was monitored after each block pair (OET, MET) and the stimulus contrast was adjusted in steps of 12.5% within the range from 25 to 100%. This manipulation was necessary to maintain overall performance in both tasks on a stable level of 50% correct responses. Between the conditions of interest (OET vs. MET), contrast and ISI were always identical.

Experimental Design.

Psychophysical threshold assessment. Before MEG recording, the participants underwent a psychophysical threshold assessment. The stimulus display was presented centrally after a fixation cross (1° DVA, 0.5-s duration) and a blank period (duration randomly jittered in steps of 10 ms between 0.5 and 1.5 s). On each trial, a randomly chosen ISI (in 10-ms steps between 30 and 90 ms) separated both displays (10-ms duration each). Participants had to indicate the target location (odd or missing element) via mouse click on a number grid (labeled 1–16) presented after 0.5 s at the prior stimulus display location. OET and MET performance was measured in separate blocks (two blocks of 70 trials each; order counterbalanced over subjects; about 10-min experiment duration). For each task, the proportion of correct responses across ISIs and the difference of the performance curves were calculated. We computed the zero crossing at the abscissa of the linear fit to the performance difference (intersection point between fits), to match performance between the tasks. The closest estimate in the range of the tested ISIs (30–90 ms in steps of 10 ms) was selected for each participant. Each subject was then run with his/her individually adjusted, performance-matching ISI held constant in the MEG experiment. Stimuli therefore differed between subjects in objective, physical duration but instead were equated on a given level of task difficulty at the subject-specific, psychophysical threshold. Linear curve fitting yielded an average intersection point of 68 ± 27 ms (SD) and sufficiently good fits (MET: $R^2 = 0.93$; OET: $R^2 = 0.9$). Post hoc analysis revealed that a sigmoid function accounted slightly better for the observed data. Thus, sigmoid curve fitting was used for the later correlation analysis (*Behavioral Data Analysis*).

Main MEG experiment. In the MEG experiment, the stimulus display was presented centrally after a fixation cross (1° DVA, 0.5-s duration) and a blank period (duration randomly jittered between 0.5 and 1.5 s in steps of 10 ms). On each trial, a subject-specific ISI (ranging between 40 and 90 ms across subjects) separated both displays (10-ms duration each). Participants had to indicate the target location (odd or missing element) via mouse click on a number grid (labeled 1–16) presented 0.5 s after the disappearance of the second stimulus frame (Fig. 1*D*). The OET and MET were tested in separate blocks (10 blocks of 50 trials each, order counterbalanced over subjects). The experiment lasted about 1 h.

Behavioral Data Analysis. The main aim of the threshold assessment before the main experiment was to match performance between the two tasks during MEG recording by choosing a fixed ISI for each participant (Fig. 1*C*). A second aim was to capture a behavioral index of task performance for each participant. To this end, the psychometric curves as a function of ISI were fitted with a generalized logistic function with four free parameters (sigmoid *S*, Eq. **1**):

$$S = (A + B) \Big/ \left(1 + e^{-(x-C)/D}\right). \quad [1]$$

On average, a sigmoid function accounted very well for the observed data (MET: $R^2 = 0.93$; OET: $R^2 = 0.94$; Fig. 1*B*). The psychometric curve fits for each participant can be seen in Fig. S6. Overall, the psychometric curve fits yielded the expected pattern of increasing segregation performance and decreasing integration performance with longer ISIs. We determined the ISI, at which each psychometric curve for each participant was closest to 50% correct trials. The possible ISI thresholds were restricted to the range between 10 and 100 ms, such that more extreme values were cut off at these bounds. Values outside this range occurred in 13% of the cases. Negative or very high values occur when participants are biased toward one or the other task (intercept shift), such that their 50% point was not accurately assessed within the range of ISIs tested. Choosing the closest extreme ISI value maintains the effects in an interpretable range (outlier correction) and accounts for idiosyncratic biases by preserving the order of the expected effects (i.e., short threshold for above 50% OET performance with short ISIs, long threshold for below 50% OET performance with long ISIs, and vice versa for the MET). For one participant, performance did not follow the expected sigmoidal pattern: it was low for segregation for all tested ISIs and a sigmoid fit did not yield a monotonic increase with ISI. This participant was run with the longest possible ISI (90 ms) during the MEG experiment and was excluded from the correlation analysis based on the 50% point of the sigmoid fit.

All error bars (for both behavioral and MEG measures) show the SEM for repeated measures. The mean between conditions was subtracted from the data in each condition before calculating the SE. The resulting error estimate was bias corrected by the number of conditions [*M*, multiplied by $\sqrt{(M/(M-1))}$] (42).

MEG Data Analysis.

Data preprocessing. The data were analyzed using custom-built MATLAB code (MATLAB 8.2; MathWorks) and the FieldTrip toolbox (43). Data were segmented from 1.5 s before to 1.5 s after display 1 onset and down-sampled off-line to 250 Hz. Data were bandpass filtered between 1 and 100 Hz and band-stop filtered between 49 and 51 Hz with a two-pass Butterworth filter (order 4), applied in the forward and reverse directions. Only magnetometer information was used for all reported analyses. Unless otherwise indicated, the trial average was subtracted from each single trial, to obtain induced activity without the contribution from stimulus-evoked components (except for the instantaneous frequency analysis for evoked activity; Fig. S1). The conditions of interest (OET, MET) were equated in trial number by drawing a random subsample of trials equal to the minimum trial number across conditions. The number of presented trials for each condition was equal by experimental design (250 trials; see above), but the artifact rejection procedure (see below) introduced small deviations between conditions.

Instantaneous frequency. We calculated a time-varying estimate of the instantaneous alpha frequency following previously published procedures (9, 23). First, single-trial MEG data were bandpass filtered with a zero-phase, plateau-shaped FIR filter (forward and reverse direction; filter order 94; 15%, transition width). Different cutoff frequencies were chosen for the different frequency bands [alpha: 8–12 or 8–15 Hz (for the control analysis, see Fig. S9); delta: 1–3 Hz; theta: 3–7 Hz; beta: 15–30 Hz; gamma: 30–50 Hz]. The Hilbert transform was used to compute the instantaneous phase angle over time. The instantaneous frequency is defined as the time rate of change of the instantaneous phase angle. Thus, the temporal derivate of the instantaneous Hilbert phase corresponds to the instantaneous frequency in hertz (when scaled by the sampling rate and 2*pi). The phase angle time series is prone to noise that can cause sharp, nonphysiological responses in its derivative. Thus, the instantaneous frequency estimate was filtered 10 times with a median filter (10 equally spaced window sizes between 10 and 400 ms). Finally, the median instantaneous frequency estimate across the different median-filter windows was calculated and selected as the instantaneous frequency per subject.

Statistical analysis was done on sensor-level data, unless otherwise indicated. The average instantaneous alpha frequency over trials was compared between conditions (OET vs. MET) for the time interval between −0.5 and 0.5 s around display 1 onset, using a nonparametric, cluster-based permutation test (44). This procedure controls for the type I error accumulation arising from multiple statistical comparisons at multiple time points and sensors. First, spatiotemporal clusters of adjacent suprathreshold effects (dependent-samples *t* statistics exceeding $P < 0.05$, two-sided) were identified. The *t* values within a connected cluster were summed up as a cluster-level statistic. Then, random permutations of the data were drawn by exchanging the data between conditions within the participants. After each permutation run, the maximum cluster-level statistic was recorded, generating a reference distribution of cluster-level statistics (approximated with a Monte Carlo procedure of 1,000 permutations). The proportion of values in the corresponding reference distribution that exceeded the observed cluster statistic yielded an estimated cluster-level *P* value, which is corrected for multiple comparisons (Fig. 2 *A* and *B* and Fig. S1). The resulting significant channel cluster for the alpha band was selected as channels of interest for subsequent analyses. In addition to the cluster-based permutation test, the contrast OET vs. MET was tested for alpha, delta, theta, beta, and gamma frequencies with dependent-samples *t* tests [averaged over the channels of interest and between −0.3 and 0 s (prestimulus) and 0 and 0.3 s (poststimulus)]. Fig. 3*C* shows the instantaneous frequency difference between tasks (OET − MET) for each frequency band and time epoch.

The time courses were aligned to display 1 onset for the main analyses. Instead, Fig. S8 shows the instantaneous alpha frequency time courses aligned to the offset of the fixation cross on each trial. We used the cluster-based permutation procedure to test for differences in alpha frequency modulation between tasks for the interval from 0.5 to 1.5 s after fixation offset [averaged over the significant sensors for the instantaneous frequency analysis (26 magnetometer sensors; Fig. 2*B*)]. This covers the entire range of possible stimulus onsets, which were randomly jittered on each trial (*Experimental Design*). Fig. S8 *B* and *C* shows the instantaneous alpha frequency aligned to fixation offset separately for trials with early and later stimulus onsets (above/below 1 s of prestimulus jitter).

Frequency peak detection. Each participant's peak alpha frequency was determined for the prestimulus and poststimulus time epoch. To this end, a Fourier analysis (FFT) in the range between 1 and 50 Hz was applied to two 0.5-s-long time epochs before or after display 1 onset (−0.5–0 s/0–0.5 s). The epochs were Hanning-tapered and zero-padded to a length of 10 s, to obtain a sufficiently good frequency resolution (0.1 Hz). Frequency peak detection for the resulting power spectra was performed on the significant sensors for the instantaneous frequency analysis (26 magnetometer sensors; Fig. 2*B*). For each participant and sensor of interest, we identified the local maximum in the power spectrum in the range between 8 and 15 Hz (MATLAB function findpeaks.m). In case no local maximum was detected, we inserted "NaN." On average, this happened on 14.8% of the cases (±12.7% SD). We chose the frequency band of interest to span between 8 and 15 Hz, because individual subjects showed clear peaks in this range (Figs. S3 and S4). This choice corresponds with recent reports about individual differences

in the peak alpha frequency (45). Alpha peaks were averaged over sensors and compared between conditions (OET vs. MET, prestimulus and poststimulus epoch) with a two-way, repeated-measures analysis of variance (2 × 2 ANOVA) and dependent-samples *t* tests (Fig. 3*A*).

Correlation between behavioral thresholds and instantaneous frequency. We tested the relationship between the behavioral task thresholds and the participant's instantaneous alpha frequency. The behavioral variables were calculated as described in *Behavioral Data Analysis* (ISI with 50% correct responses based on the sigmoid curve fit to OET/MET performance). Each participant's peak instantaneous alpha frequency (averaged between tasks) and the difference in instantaneous alpha frequency (OET − MET) were averaged over the significant sensors for the instantaneous frequency analysis (26 magnetometer sensors of interest; Fig. 2*B*). The Pearson correlation between behavioral thresholds and frequency measures across participants was calculated on a time point-by-time point basis and tested for significance in the 0.5-s time epoch following display 1 onset (0–0.5 s). To correct for multiple comparisons at multiple time samples, we used the nonparametric, cluster-based permutation test (44) (see above). Fig. S7 shows the time course for each correlation. Fig. 4 *B* and *C* shows behavioral thresholds plotted against frequency measures averaged over (marginally) significant time epochs and the corresponding MEG sensor topographies.

Correct vs. incorrect trials. We compared the difference in instantaneous alpha frequency between tasks (OET vs. MET) separately for correct and incorrect trials. The conditions of interest (correct/incorrect trials for OET/MET) were equated in trial number by drawing a random subsample of trials equal to the minimum trial number across conditions. This process was repeated 500 times and then averaged across the trial subsamples. This yielded a final, representative time course per condition. The difference between tasks for correct or incorrect trials averaged over the significant sensors from the initial instantaneous frequency analysis (26 magnetometer sensors of interest; Fig. 2*B*) was then quantified with a dependent-samples *t* test. A nonparametric, cluster-based permutation procedure (44) was used to correct for multiple comparisons within the time interval between −0.5 to +0.5 s relative to display 1 onset.

We tested whether the onset of the alpha frequency difference between tasks occurred at different times (relative to stimulus onset) for correct and incorrect trials. For each subject, we conducted a one-tailed, independent-samples *t* test testing whether single-trial frequencies were higher in the OET compared with the MET task ($P < 0.05$), separately for correct and incorrect trials. We then saved the earliest time point of significant differences (time to significance) and the associated *t* value for each subject. The conditions of interest (correct/incorrect trials for OET/MET) were equated in trial number (see above), to ensure that each *t* statistic was based on the same degrees of freedom. This procedure was repeated 500 times. We then calculated the median time to significance and *t* value across the trial subsamples to derive a final, representative estimate. For trial subsamples for which no time points were significant, we used the point with the smallest *P* value (note that the results were the same when we inserted "NaN" in those instances). We then compared the time-to-significance metric across subjects between correct and incorrect trials using a nonparametric Wilcoxon sign-rank test.

Supporting Information. See *Supporting Information* for details on the MEG and stimulus presentation apparatus, artifact rejection and source reconstruction pipelines, and time–frequency power analysis.

ACKNOWLEDGMENTS. This research was supported by a European Research Council Grant, "Construction of Perceptual Space-Time" (StG Agreement 313658).

1. Varela FJ, Toro A, John ER, Schwartz EL (1981) Perceptual framing and cortical alpha rhythm. *Neuropsychologia* 19:675–686.
2. Cecere R, Rees G, Romei V (2015) Individual differences in alpha frequency drive crossmodal illusory perception. *Curr Biol* 25:231–235.
3. Cravo AM, Santos KM, Reyes MB, Caetano MS, Claessens PME (2015) Visual causality judgments correlate with the phase of alpha oscillations. *J Cogn Neurosci* 27:1887–1894.
4. Milton A, Pleydell-Pearce CW (2016) The phase of pre-stimulus alpha oscillations influences the visual perception of stimulus timing. *Neuroimage* 133:53–61.
5. Kristofferson AB (1967) Successiveness discrimination as a two-state, quantal process. *Science* 158:1337–1339.
6. Wutz A, Weisz N, Braun C, Melcher D (2014) Temporal windows in visual processing: "Prestimulus brain state" and "poststimulus phase reset" segregate visual transients on different temporal scales. *J Neurosci* 34:1554–1565.
7. VanRullen R (2016) Perceptual cycles. *Trends Cogn Sci* 20:723–735.
8. Gho M, Varela FJ (1988–1989) A quantitative assessment of the dependency of the visual temporal frame upon the cortical rhythm. *J Physiol (Paris)* 83:95–101.
9. Samaha J, Postle BR (2015) The speed of alpha-band oscillations predicts the temporal resolution of visual perception. *Curr Biol* 25:2985–2990.
10. Minami S, Amano K (2017) Illusory jitter perceived at the frequency of alpha oscillations. *Curr Biol* 27:2344–2351.e4.
11. Yeshurun Y, Levy L (2003) Transient spatial attention degrades temporal resolution. *Psychol Sci* 14:225–231.
12. Correa A, Sanabria D, Spence C, Tudela P, Lupiáñez J (2006) Selective temporal attention enhances the temporal resolution of visual perception: Evidence from a temporal order judgment task. *Brain Res* 1070:202–205.
13. Bausenhart KM, Rolke B, Ulrich R (2008) Temporal preparation improves temporal resolution: Evidence from constant foreperiods. *Percept Psychophys* 70:1504–1514.
14. Samaha J, Bauer P, Cimaroli S, Postle BR (2015) Top-down control of the phase of alpha-band oscillations as a mechanism for temporal prediction. *Proc Natl Acad Sci USA* 112:8439–8444.
15. Bonnefond M, Jensen O (2012) Alpha oscillations serve to protect working memory maintenance against anticipated distracters. *Curr Biol* 22:1969–1974.
16. Samaha J, Sprague TC, Postle BR (2016) Decoding and reconstructing the focus of spatial attention from the topography of alpha-band oscillations. *J Cogn Neurosci* 28:1090–1097.
17. Worden MS, Foxe JJ, Wang N, Simpson GV (2000) Anticipatory biasing of visuospatial attention indexed by retinotopically specific α-band electroencephalography increases over occipital cortex. *J Neurosci* 20:RC63.
18. Sauseng P, et al. (2005) A shift of visual spatial attention is selectively associated with human EEG alpha activity. *Eur J Neurosci* 22:2917–2926.
19. Hogben JH, di Lollo V (1974) Perceptual integration and perceptual segregation of brief visual stimuli. *Vision Res* 14:1059–1069.
20. Wutz A, Muschter E, van Koningsbruggen MG, Weisz N, Melcher D (2016) Temporal integration windows in neural processing and perception aligned to saccadic eye movements. *Curr Biol* 26:1659–1668.
21. Iemi L, Chaumon M, Crouzet SM, Busch NA (2017) Spontaneous neural oscillations bias perception by modulating baseline excitability. *J Neurosci* 37:807–819.
22. Samaha J, Iemi L, Postle BR (2017) Prestimulus alpha-band power biases visual discrimination confidence, but not accuracy. *Conscious Cogn* 54:47–55.
23. Cohen MX (2014) Fluctuations in oscillation frequency control spike timing and coordinate neural networks. *J Neurosci* 34:8988–8998.
24. Samaha J, Gosseries O, Postle BR (2017) Distinct oscillatory frequencies underlie excitability of human occipital and parietal cortex. *J Neurosci* 37:2824–2833.
25. Schroeder CE, Lakatos P (2009) Low-frequency neuronal oscillations as instruments of sensory selection. *Trends Neurosci* 32:9–18.
26. Engel AK, Fries P (2010) Beta-band oscillations—signalling the status quo? *Curr Opin Neurobiol* 20:156–165.
27. Buschman TJ, Miller EK (2007) Top-down versus bottom-up control of attention in the prefrontal and posterior parietal cortices. *Science* 315:1860–1862.
28. van Diepen RM, Cohen MX, Denys D, Mazaheri A (2015) Attention and temporal expectations modulate power, not phase, of ongoing alpha oscillations. *J Cogn Neurosci* 27:1573–1586.
29. Hughes SW, et al. (2004) Synchronized oscillations at α and θ frequencies in the lateral geniculate nucleus. *Neuron* 42:253–268.
30. Hughes SW, Crunelli V (2005) Thalamic mechanisms of EEG alpha rhythms and their pathological implications. *Neuroscientist* 11:357–372.
31. Hughes SW, et al. (2011) Thalamic gap junctions control local neuronal synchrony and influence macroscopic oscillation amplitude during EEG alpha rhythms. *Front Psychol* 2:193.
32. Lőrincz ML, Kékesi KA, Juhász G, Crunelli V, Hughes SW (2009) Temporal framing of thalamic relay-mode firing by phasic inhibition during the alpha rhythm. *Neuron* 63:683–696.
33. Wimmer RD, et al. (2015) Thalamic control of sensory selection in divided attention. *Nature* 526:705–709.
34. McAlonan K, Cavanaugh J, Wurtz RH (2008) Guarding the gateway to cortex with attention in visual thalamus. *Nature* 456:391–394.
35. Phillips JM, Kambi NA, Saalmann YB (2016) A subcortical pathway for rapid, goal-driven, attentional filtering. *Trends Neurosci* 39:49–51.
36. Bollimunta A, Chen Y, Schroeder CE, Ding M (2008) Neuronal mechanisms of cortical alpha oscillations in awake-behaving macaques. *J Neurosci* 28:9976–9988.
37. Silva LR, Amitai Y, Connors BW (1991) Intrinsic oscillations of neocortex generated by layer 5 pyramidal neurons. *Science* 251:432–435.
38. Flint AC, Connors BW (1996) Two types of network oscillations in neocortex mediated by distinct glutamate receptor subtypes and neuronal populations. *J Neurophysiol* 75:951–957.
39. Morishima Y, et al. (2009) Task-specific signal transmission from prefrontal cortex in visual selective attention. *Nat Neurosci* 12:85–91.
40. Squire RF, Noudoost B, Schafer RJ, Moore T (2013) Prefrontal contributions to visual selective attention. *Annu Rev Neurosci* 36:451–466.
41. Di Lollo V (1977) Temporal characteristics of iconic memory. *Nature* 267:241–243.
42. Morey RD (2008) Confidence intervals from normalized data: A correction to Cousineau (2005). *Tutor Quant Methods Psychol* 4:61–64.
43. Oostenveld R, Fries P, Maris E, Schoffelen J-M (2011) FieldTrip: Open source software for advanced analysis of MEG, EEG, and invasive electrophysiological data. *Comput Intell Neurosci* 2011:156869.
44. Maris E, Oostenveld R (2007) Nonparametric statistical testing of EEG- and MEG-data. *J Neurosci Methods* 164:177–190.
45. Haegens S, Cousijn H, Wallis G, Harrison PJ, Nobre AC (2014) Inter- and intra-individual variability in alpha peak frequency. *Neuroimage* 92:46–55.
46. Brainard DH (1997) The Psychophysics Toolbox. *Spat Vis* 10:433–436.
47. Pelli DG (1997) The VideoToolbox software for visual psychophysics: Transforming numbers into movies. *Spat Vis* 10:437–442.
48. Van Veen BD, van Drongelen W, Yuchtman M, Suzuki A (1997) Localization of brain electrical activity via linearly constrained minimum variance spatial filtering. *IEEE Trans Biomed Eng* 44:867–880.